
Evidence on the regularization properties of Maximum-Entropy Reinforcement Learning

Anonymous Author(s)

Affiliation

Address

email

Abstract

1 The generalisation and robustness properties of policies learnt through Maximum-
2 Entropy Reinforcement Learning are investigated on chaotic dynamical systems
3 with Gaussian noise on the observable. First, the robustness under noise contamina-
4 tion of the agent’s observation of entropy regularised policies is observed. Second,
5 notions of statistical learning theory, such as complexity measures on the learnt
6 model, are borrowed to explain and predict the phenomenon. Results show the
7 existence of a relationship between entropy-regularised policy optimisation and
8 robustness to noise, which can be described by the chosen complexity measures.

9 1 Introduction

10 Maximum-Entropy Reinforcement Learning [Williams et al., 1991] aims to solve the problem of
11 learning a policy which optimises a chosen utility criterion while promoting the entropy of the policy.
12 The standard way to account for the constraint is to add a Lagrangian term to the objective function.
13 This entropy-augmented objective is commonly referred to as the soft objective.

14 There are multiple advantages in solving the soft objective over the standard objective. For in-
15 stance, favouring stochastic policies over deterministic ones allows learning multi-modal distribu-
16 tions [Haarnoja et al., 2017]. In addition, agent stochasticity is a suitable way to deal with uncertainty
17 induced by Partially Observable Markov Decision Processes (PO-MDP). Indeed, there are PO-MDP
18 such that the best stochastic adapted policy can be arbitrarily better than the best deterministic adapted
19 policy [Sigaud and Buffet, 2010]¹.

20 Furthermore, several important works highlight both theoretical and experimental *robustness* of those
21 policies under noisy dynamics and rewards [Eysenbach and Levine, 2022].

22 Related to the latter notion of robustness, the maximum-entropy principle exhibits non-trivial general-
23 isation capabilities, which are desired in real-world applications [Haarnoja et al., 2018].

24 However, the reasons for such robustness properties are not yet well understood. Thus, further
25 investigations are needed to grasp the potential of the approach and to design endowed algorithms. A
26 clear connection between Maximum-Entropy RL and their robustness properties is important and
27 intriguing.

28 Meanwhile, recent work in the deep learning community discusses how some complexity measures
29 on the neural network model are related to generalisation, and explain typically observed phenom-
30 ena [Neyshabur et al., 2017]. In fact, these complexity measures are derived from the learnt model,

¹In this context, the term “stochastic adapted policy” is a conditional distribution on the control space \mathcal{U} given the observation space \mathcal{Y} since this type of policy is “adapted” from Markovian policies in fully observable MDPs.

31 bound the PAC-Bayes generalisation error, and are meant to identify which of the local minima
32 generalise well.

33 As a matter of fact, a relatively recent trend in statistical learning suggests generalisation is not only
34 favored by the regularisation techniques (*e.g.*, dropout) but mainly because of the flatness of the local
35 minima [Hochreiter and Schmidhuber, 1997, Dinh et al., 2017, Keskar et al., 2017]. The reasons for
36 such regularity properties remain an open problem. This work aims to address these points in the
37 context of Reinforcement Learning, and addresses the following questions:

38 *What is the bias introduced by entropy regularisation? Are the aforementioned complexity measures*
39 *also related to the robustness of the learnt solutions in the context of Reinforcement Learning?*

40 In that respect, by defining a notion of robustness against noisy contamination of the observable,
41 a study on the impact of the entropy regularisation on the robustness of the learnt policies is first
42 conducted. After explaining the rationale behind the choice of the complexity measures, a numerical
43 study is performed to validate the hypothesis that some measures of complexity are good robustness
44 predictors. Finally, a link between the entropy regularisation and the flatness of the local minima is
45 treated through the information geometry notion of Fisher Information.

46 The paper is organised as follows. Section 2 introduces the background and related work, Section 3
47 presents the problem setting. Section 4 is the core contribution of this paper. This section introduces
48 the rationale behind the studied complexity measures from a learning theory perspective, as well
49 as their expected relation to robustness. Lastly, Section 5 presents the experiments related to the
50 policy robustness as well as their complexity, while Section 6 examines the results obtained. Finally,
51 Section 7 concludes the paper.

52 2 Related work

53 **Maximum Entropy Policy Optimisation** In Haarnoja et al. [2018], the generalisation capabilities
54 of entropy-based policies are observed where multimodal policies lead to optimal solutions. It is
55 suggested that maximum entropy solutions aim to learn all the possible ways to solve a task. Hence,
56 transfer learning to more challenging objectives is made easier, as demonstrated in their experiment.
57 This study investigates the impact of adopting policies with greater randomness on their robustness.
58 The impact of the entropy regularisation on the loss landscape has been recently studied in Ahmed
59 et al. [2019]. They provide experimental evidence about the smoothing effect of entropy on the
60 optimisation landscape. The present study aims specifically to answer the question in Section 3.2.4
61 of their paper: *Why do high entropy policies learn better final solutions?* This paper extends their
62 results from a complexity measure point of view. Recently, Neu et al. [2017], Derman et al. [2021]
63 studied the equivalence between robustness and entropy regularisation on regularised MDP.

64 **Flat minima and Regularity** The notion of local minima flatness was first introduced in the context
65 of supervised learning by Hochreiter and Schmidhuber [1997] through the Gibbs formalism [Haussler
66 and Oppel, 1997]. Progressively, different authors stated the concept with geometric tools such as first
67 order (gradient) or second order (Hessian) regularity measures [Zhao et al., 2022, Keskar et al., 2017,
68 Sagun et al., 2017, Yoshida and Miyato, 2017, Dinh et al., 2017]. In a similar fashion, Chaudhari
69 et al. [2019] uses the concept of local entropy to smooth the objective function.

70 In the scope of Reinforcement Learning, Ahmed et al. [2019] observed that flat minima characterise
71 maximum entropy solutions, and entropy regularisation has a smoothing effect on the loss landscape,
72 reducing the number of local optima. A central objective of this present study is to investigate this
73 latter property further and relate it to the field of research on robust optimisation. Lastly, among the
74 few recent studies on the learning and optimisation aspects of RL, Gogianu et al. [2021] shows how a
75 well-chosen regularisation can be very effective for deep RL. Indeed, they explain that constraining
76 the Lipschitz constant of only one neural network layer is enough to compete with state-of-the-art
77 performances on a standard benchmark.

78 **Robust Reinforcement Learning** A branch of research related to this work is the study of robust-
79 ness with respect to the uncertainty of the dynamics, namely *Robust Reinforcement Learning* (Robust
80 RL), which dates back to the 1970s [Satia and Lave, 1973]. Correspondingly, in the field of control
81 theory, echoes the notion of robust control and especially H_∞ control [Zhou et al., 1996], which
82 also appeared in the mid-1970s after observing Linear Quadratic Regulator (LQR) solutions are very

83 sensitive to perturbations while not giving consistent enough guarantees [Doyle, 1996].
84 More specifically, the Robust RL paradigm aims to control the dynamics in the worst-case sce-
85 nario, *i.e.*, to optimise the minimal performance for a given objective function over a set of possible
86 dynamics through a min-max problem formulation. This set is often called *ambiguity set* in the
87 literature. It is defined as a region in the space of dynamics close enough w.r.t. to some divergence
88 measure, such as the relative entropy [Nilim and Ghaoui, 2003]. Closer to this work, the recent paper
89 from Eysenbach and Levine [2022] shows theoretically how Maximum-Entropy RL policies are
90 inherently robust to a certain class of dynamics of fully-observed MDP. The finding of their article
91 might still hold in the partially observable setting as any PO-MDP can be cast as fully-observed MDP
92 with a larger state-space of probability measures [Hernández-Lerma and Lasserre, 1996], providing
93 the ambiguity set is adapted to a more complicated space.

94 3 Problem Setup and Background

95 3.1 Partially Observable Markov Decision Process with Gaussian noise

96 First, the control problem when noisy observations are available to the agent is formulated. The study
97 focuses on *Partially Observable Markov Decision Processes (PO-MDP)* with Gaussian noise of the
98 form [Deisenroth and Peters, 2012]:

$$\begin{aligned} X_{h+1} &= F(X_h, U_h) \\ Y_h &= G(X_h) + \epsilon, \quad \epsilon \sim \mathcal{N}(0, \sigma_Y^2 I_d) \end{aligned} \quad (1)$$

99 with $X_h \in \mathcal{X}$, $U_h \in \mathcal{U}$ and $Y_h \in \mathcal{Y}$ for any $h \in \mathbb{N}$, where \mathcal{X} , \mathcal{U} and \mathcal{Y} are respectively the
100 corresponding state, action and observation spaces. The initial state starts from a reference state
101 x_e^* on which centred Gaussian noise with diagonal covariance $\sigma_e^2 I_d$ is additively applied, $X_0 \sim$
102 $\mathcal{N}(x_e^*, \sigma_e^2 I_d)$. Associated with the dynamics, an instantaneous cost function $c : \mathcal{X} \times \mathcal{U} \rightarrow \mathbb{R}_+$ is also
103 given to define the control model.

104 In this context, a *policy* π is a transition kernel on \mathcal{A} given \mathcal{Y} , *i.e.*, a distribution on actions conditioned
105 on observations. This kind of policies are commonly used in the literature but can be very poor in
106 the partially observable setting where information is missing. Together, a control model, a policy
107 π and an initial distribution P_{X_0} on \mathcal{X} define a stochastic process with distribution $P^{\pi, \epsilon}$ where the
108 superscript ϵ highlights the dependency on the observation noise ϵ . Similarly, one denotes by P^π the
109 distribution of the process when the noise is zero almost-surely, *i.e.*, $P^\pi = P^{\pi, 0}$. More details about
110 the PO-MDP control problem can be found in Hernández-Lerma and Lasserre [1996], Cassandra
111 [1998].

112 Here, the maximum-entropy control problem is to find a policy π^* which minimises the following
113 performance criterion

$$J_m^{\pi, \epsilon} = \mathbb{E}^{\pi, \epsilon} \left[\sum_{h=0}^H \gamma^h c(X_h, U_h) \right] + \alpha_m \mathbb{E}^{\pi, \epsilon} \left[\sum_{h=0}^H \gamma^h \mathcal{H}(\pi(\cdot | X_h)) \right], \quad (2)$$

114 where $H \in \mathbb{N}$ is a given time horizon, $\mathbb{E}^{\pi, \epsilon}$ denotes the expectation under the probability measure
115 $P^{\pi, \epsilon}$, \mathcal{H} denotes the differential entropy [Cover and Thomas, 2006] and α_m is a time-dependent
116 weighting parameter that evolves over training time $m \leq m_{\mathcal{D}} = |\mathcal{D}|$ with $|\mathcal{D}|$ being the total number
117 of times the agent interacts with the system such that all observations used by the learning algorithm
118 form the dataset \mathcal{D} at the end of the training procedure (when $m_{\mathcal{D}}$ environment interactions are
119 done).
120

121 $J_m^{\pi, \epsilon}$ is denoted $J^{\pi, \epsilon}$. The quantity $J^{\pi, \epsilon}$ is called the value function or, more generally, *loss*.
122 Moreover, the performance gap for dynamics with noisy and noiseless observables will be considered
123 in the sequel. In this context, the (*rate of*) *excess risk under noise* is defined as the difference between
124 the loss under noisy dynamics and the loss under noiseless dynamics:

125 **Definition 1 (Excess Risk Under Noise)** *The excess risk under noise of a policy π for a PO-MDP*
126 *with dynamics (1) is defined as:*

$$\mathcal{R}^\pi = \mathbb{E}^{\pi, \epsilon} \left[\sum_{h=0}^H \gamma^h c(X_h, U_h) \right] - \mathbb{E}^\pi \left[\sum_{h=0}^H \gamma^h c(X_h, U_h) \right] = J^{\pi, \epsilon} - J^\pi \quad (3)$$

127 Similarly, the rate of excess risk under noise is defined as:

$$\mathring{\mathcal{R}}^\pi = \frac{J^{\pi, \epsilon} - J^\pi}{J^\pi} = \frac{\mathcal{R}^\pi}{J^\pi} \quad (4)$$

128 Note that in the above definition,

129 expectations are taken with respect to the probability measure $P^{\pi, \epsilon}$ and P^π respectively. The *rate of excess risk under noise* represents the performance degradation after noise introduction in value function units. In the rest of the paper, arguments to derive complexity measures will be developed, allowing to predict the excess risk under noise and provide numerical evidence showing maximum-entropy policies are more robust regarding this metric. Hence, maximum-entropy policies implicitly learn a robust control policy in the sense of Definition 1.

135 In the next section, some concepts of statistical learning theory are introduced. Then, complexity measures will be defined to quantify the regularisation power of the maximum-entropy objective of (2).

138 4 Complexity Measures and Robustness

139 4.1 Complexity Measures

140 The principal objective of *statistical learning* is to provide bounds on the generalisation error, so-called *generalisation bounds*. In the following, it is assumed that an algorithm \mathcal{A} returns a hypothesis $\pi \in \mathcal{F}$ from a dataset \mathcal{D} . Note that the dataset \mathcal{D} is random and the algorithm \mathcal{A} is a randomised algorithm.

144 As the hypothesis set \mathcal{F} typically used in machine learning is infinite, a practical way to quantify the generalisation ability of such a set must be found. This quantification is done by introducing *complexity measures*, enabling the derivation of generalisation bounds.

147 **Definition 2 (Complexity measure)** *A complexity measure is a mapping $\mathcal{M} : \mathcal{F} \rightarrow \mathbb{R}_+$ that maps a hypothesis to a positive real number.*

149 According to Neyshabur et al. [2017] from which this formalism is inspired, an appropriate complexity measure satisfies several properties. In the case of parametric models $\pi_\theta \in \mathcal{F}(\Theta)$ with $\theta \in \Theta \subset \mathbb{R}^b$, it should increase with the dimension b of the parameter space Θ as well as being able to identify when the dataset \mathcal{D} contains totally random, spurious or adversarial data. As a result, finding good complexity measures \mathcal{M} allows the quantification of the generalisation ability of a hypothesis set \mathcal{F} or a model π and an algorithm \mathcal{A} .

155 4.2 Complexity measures for PO-MDP with Gaussian Noise

156 This paper studies heuristics about generalisation bounds on the optimal *excess risk under noise* from Definition 1 when the optimal policy π_{θ^*} is learnt with an algorithm \mathcal{A} on the non-noisy objective J^π , where $\alpha_m = 0$ for any m .

159 **Definition 3 ((Rate of) Excess Risk Under Noise Bound)** *Given an optimal policy π^* learnt with an algorithm \mathcal{A} on the non-noisy objective J^π , the optimal excess risk under noise bound is a real-valued mapping φ such that*

$$\mathcal{R}^{\pi^*} \leq \varphi(\mathcal{M}(\pi^*, \mathcal{D}), m_{\mathcal{D}}, \eta, \delta) \quad (5)$$

162 and φ is increasing with the complexity measure \mathcal{M} and the sample complexity $m_{\mathcal{D}}$. The definition is similar for the rate of excess risk under noise bound where $\mathring{\mathcal{R}}^{\pi^*}$ is used instead of \mathcal{R}^{π^*} .

164 Hence, considering a learning algorithm \mathcal{A} with a parameterised family $\mathcal{F}(\Theta) = (\pi_\theta)_{\theta \in \Theta}$, $\Theta \subset \mathbb{R}^b$, such that $\theta = (\theta_\mu, \theta_{\sigma_\pi})$ with $\pi_\theta(\cdot | x) \sim \mathcal{N}(\mu_{\theta_\mu}(x), \text{diag}(\theta_{\sigma_\pi}))$, $x \in \mathcal{X}$, - where μ_{θ_μ} is a shallow multi-layer feed-forward neural network (with depth-size $l = 2$, width $w = 64$ neurons, weights matrix $(\theta_\mu^i)_{1 \leq i \leq l}$) and $\text{diag}(\theta_{\sigma_\pi})$ is a diagonal matrix of dimension $q = \dim(\mathcal{U})$ parameterising the

168 variance² - to learn the optimal policy π_{θ^*} , multiple complexity measures \mathcal{M} are defined and details
 169 on their underlying rationale are given below.

170 4.2.1 Norm based complexity measures

171 First, the so-called norm-based complexity measures are functions of the norm of some subset of the
 172 parameters of the model. For instance, a common norm-based measure calculates the product of the
 173 operator norms of the neural network linear layers. The measures are commonly used in the statistical
 174 learning theory literature to derive bounds on the generalisation gap, especially in the context of
 175 neural networks [Neyshabur et al., 2015, Golowich et al., 2018, Miyato et al., 2018].

176 In fact, the product of the norm of the linear layers of a standard class of multi-layer neural networks
 177 (including Convolutional Neural Networks) serves as an upper bound on the often intractable Lipschitz
 178 constant of the network [Miyato et al., 2018]. Thus, controlling the magnitude of the weights of the
 179 linear layers increases the regularity of the model.

180 Consequently, the following complexity measures are defined:

- 181 • $\mathcal{M}(\pi_\theta, \mathcal{D}) = \|\theta_\mu\|_p$
- 182 • $\mathcal{M}(\pi_\theta, \mathcal{D}) = \prod_{i=1}^l \|\theta_\mu^i\|_p$ where θ_μ^i is the i^{th} layer of the network μ_{θ_μ} .

183 In this context $\|\cdot\|_p$ with $p = 1, 2, \infty$ denotes the p -operator norm while $p = F$ denotes the
 184 Frobenius norm, which is discarded for the first case of the full parameters vector θ_μ (since Frobenius
 185 norm is defined for matrix).

186 4.2.2 Flatness based complexity measures

187 On the other hand, another measure of complexity is given by the flatness of the optimisation local
 188 minimum (see Section 2 for a brief overview). As McAllester [2003], Neyshabur et al. [2017] have
 189 pointed out, the generalisation ability of a parametric solution is controlled by two key components
 190 in the context of supervised learning: the norm of the parameter vector and its flatness w.r.t. to the
 191 objective function.

192 One might wonder if a similar robustness property still holds in the setting of Reinforcement Learning.
 193 In this manner, complexity measures quantifying the flatness of the solution are needed. Concretely,
 194 the interest lies in the flatness of the local minima of the objective function J^π . As stated earlier,
 195 there are several ways to quantify the flatness of a solution with metrics derived from the gradient
 196 or curvature of the loss function at the local optimum, such as the Hessian’s largest eigenvalue -
 197 otherwise spectral norm [Keskar et al., 2017] or the trace of Hessian [Dinh et al., 2017].

198 Moreover, as discussed in Section 2, Ahmed et al. [2019] observed that *maximum entropy solutions*
 199 *are characterised by flat minima* while entropy regularisation has a smoothing effect on the loss
 200 landscape. Hence, a central objective of this present study is to investigate this latter property further
 201 and relate it to the robustness aspect of the resulting policies.

202 However, instead of dealing directly with the Hessian of the objective J^π this work proposes a
 203 measure based on the conditional Fisher Information \mathcal{I} of the policy due to its link with a notion of
 204 model regularity in the parameter space.

205 **Definition 4 (Conditional Fisher Information Matrix)** Let $x \in \mathcal{X}$ and π_θ a policy identified by
 206 its conditional density for a parameter $\theta \in \Theta \subset \mathbb{R}^b$ and suppose ρ is a distribution over \mathcal{X} . The
 207 conditional Fisher Information Matrix of the vector θ is defined under some regularity conditions as

$$\mathcal{I}(\theta) = - \mathbb{E}^{X \sim \rho, U \sim \pi_\theta(\cdot | X)} \left[\nabla_\theta^2 \log \pi_\theta(U | X) \right], \quad (6)$$

208 where ∇_θ^2 denotes the Hessian matrix evaluated at θ .

209 Note that the distribution over states ρ is arbitrary and can be chosen as the discounted state visitation
 210 measure ρ^π induced by the policy π [Agarwal et al., 2019] or the stationary distribution of the induced
 211 Markov process if the policy is Markovian and the MDP ergodic³ as it is done in Kakade [2001].

²Note this choice of state-independent policy variance is inspired by Ahmed et al. [2019] and simplifies the problem.

³With these choices, the following holds: $\mathbb{E}^{\rho^\pi(d_s)\pi(da|s)} = \mathbb{E}^\pi$ up to taking the expectation w.r.t. the state-action space (no subscript under X and U) or the trajectory space (with subscripts such as X_h and U_h as trajectory coordinate) Agarwal et al. [2019].

212 As a matter of fact, it has already been mentioned in the early works of policy optimisation [Kakade,
 213 2001] that this quantity \mathcal{I} might be related to the Hessian of the objective function. Indeed, the
 214 Hessian matrix of the standard objective function reads (see Shen et al. [2019] for a proof):

$$\nabla_{\theta}^2 J^{\pi_{\theta}} = \mathbb{E}^{\pi_{\theta}} \left[\sum_{h,i,j=0}^H c(X_h, U_h) \left(\nabla_{\theta} \log \pi_{\theta}(U_i | X_i) \nabla_{\theta} \log \pi_{\theta}(U_j | X_j)^T + \nabla_{\theta}^2 [\log \pi_{\theta}(U_i | X_i)] \right) \right]. \quad (7)$$

215 As suggested by the author mentioned above (S. Kakade), (7) might be related to \mathcal{I} although being
 216 weighted by the cost c . Indeed, the Hessian of the state-conditional log-likelihoods ($\nabla_{\theta}^2 \log \pi_{\theta}$ on the
 217 rightmost part of the expectation of (7)) belongs to the objective-function Hessian $\nabla_{\theta}^2 J^{\pi_{\theta}}$ while the
 218 Fisher Information $\mathcal{I}(\theta)$ is an average of the Hessian of the policy log-likelihood.

219 In any case, the conditional FIM measures the regularity of a critical component of the objective to
 220 be minimised. Thus, the trace of the conditional FIM of the mean actor network parameter θ_{μ} is
 221 suggested as a complexity measure

$$\bullet \mathcal{M}(\pi_{\theta}, \mathcal{D}) = \text{Tr}(\mathcal{I}(\theta_{\mu})) = \text{Tr}(-\mathbb{E}^{X \sim \rho^{\pi}, U \sim \pi_{\theta}(\cdot|X)} [\nabla_{\theta_{\mu}}^2 \log \pi_{\theta}(U | X)]).$$

223 Moreover, in the context of classification, a link between the degree of stochasticity of optimisation
 224 gradients (leading to flatter minima [Mulayoff and Michaeli, 2020, Xie et al., 2021]) and the FIM
 225 trace during training has recently been revealed in Jastrzebski et al. [2021]. Magnitudes of the FIM
 226 eigenvalues may be related to loss flatness and norm-based capacity measures to generalisation
 227 ability [Karakida et al., 2019] in deep learning.

228 5 Experiments

229 5.1 Robustness under noise of Maximum Entropy Policies

230 The first hypothesis is that maximum entropy policies are more robust to noise than those trained
 231 without entropy regularisation (which play the role of control experiments). Consequently, the
 232 robustness of the controlled policy π_{θ^*} is compared with the robustness of the maximum entropy
 233 policy $\pi_{\theta^*}^{\alpha}$ for different temperature evolutions $\alpha = (\alpha_m)_{0 \leq m \leq m_{\mathcal{D}}}$. In this view, and since inter-
 234 algorithm comparisons are characterised by high uncertainty [Henderson et al., 2018, Colas et al.,
 235 2018, Agarwal et al., 2021], only one algorithm \mathcal{A} (*Proximal Policy Optimisation* (PPO) Schulman
 236 et al. [2017]) is retained while results on multiple entropy constraint levels $\alpha = (\alpha_m)_{0 \leq m \leq m_{\mathcal{D}}}$ are
 237 examined.

238 In this regard, ten independent PPO models are trained for each of the five arbitrarily chosen entropy
 239 temperatures $\alpha^i = (\alpha_m^i)_{0 \leq m \leq m_{\mathcal{D}}}$ where $i \in \{1, \dots, 5\}$, on dynamics without observation noise, *i.e.*,
 240 where $\sigma_Y^2 = 0$. The entropy coefficients linearly decay during training, and all vanish ($\alpha_m = 0$) when
 241 m reaches one-fourth of the training time $m_{1/4} = \lfloor \frac{m_{\mathcal{D}}}{4} \rfloor$ in order to replicate a sort of exploration-
 242 exploitation procedure, ensuring that all objectives J_m^{π} are the same whenever $m \geq m_{1/4}$, *i.e.*,
 243 $J_m^{\pi} = J^{\pi}$. This choice is different but inspired by Ahmed et al. [2019] as they optimise using only
 244 the *policy gradient* and manipulate the standard deviation of Gaussian policies directly, whereas, in
 245 the present approach, it is done implicitly with an adaptive entropy coefficient. An algorithm that
 246 learns a model with a given entropy coefficient $\alpha = (\alpha_m)_{0 \leq m \leq m_{\mathcal{D}}}$ is denoted as \mathcal{A}_{α} .

247 The chosen chaotic systems are the *Lorenz* [Vincent and Yu, 1991] (with $m_{\mathcal{D}} = 10^6$) and *Kuramoto-*
 248 *Sivashinsky (KS)* [Bucci et al., 2019] (with $m_{\mathcal{D}} = 2 \cdot 10^6$) controlled differential equations. The
 249 defaults training hyper-parameters from *Stable-Baselines3* [Raffin et al., 2021] are used.

250 5.2 Robustness against Complexity Measures

251 So far, three separate analyses on the 5×10 models obtained have been performed on the *Lorenz*
 252 and *Kuramoto-Sivashinsky (KS)* controlled differential equations.

253 First, as mentioned before, the robustness of the models for each of the chosen entropy temperatures
 254 α^i is tested against the same dynamics but now with a noisy observable, *i.e.*, $\sigma_Y > 0$. Second,
 255 norm-based complexity measures introduced in Section 4.2 are evaluated and compared to the
 256 generalisation performances of the distinct algorithms \mathcal{A}_{α} . Third, numerical computation of the

257 conditional distribution of the trace of the Fisher Information Matrix given by (6) is performed to test
 258 the hypothesis that this regularity measure is an indicator of robust solutions. The state distribution
 259 ρ^{π_θ} is naturally chosen as the state visitation distribution induced by the policy π_θ . The following
 260 section discusses the results of those experiments.

261 6 Results

262 This section provides numerical evidence of maximum entropy’s effect on the robustness, as defined
 263 by the Excess Risk Under Noise defined by (3). Then, after quantifying robustness, the relation
 264 between the complexity measures defined in Section 4.2 and robustness is studied.

265 6.1 Entropy Regularisation induces noise robustness

266 In the first place, a distributional representation⁴ of the rate of excess risk under noise defined in (3)
 267 is computed for each of the 5×10 models obtained with the PPO algorithm \mathcal{A}_{α^i} , $i \in \{1, \dots, 5\}$ and
 268 different levels of observation noise $\sigma_Y > 0$.

269 First and foremost, the results shown in Figure 1 indicate that the noise introduction to the system
 270 observable Y of KS and Lorenz leads to a global decrease in performance, as expected.

271 The robustness to noise contamination of the two systems is improved by initialising the policy
 272 optimisation procedure up to a certain intermediate threshold of the entropy coefficient $\alpha^i > 0$. Once
 273 this value is reached, two respective behaviours are observed depending on the system. In the case of
 274 the Lorenz dynamics, the robustness continues to improve after this entropy threshold, whereas the
 275 opposite trend is observed for KS (particularly with the maximal entropy coefficient chosen).

276 Hence, the sole introduction of entropy-regularisation in the objective function impacts the robustness.
 277 This behaviour difference between Lorenz and KS might be explained by the variability of the
 278 optimisation landscapes that can be observed with respect to the chosen underlying dynamics as
 279 underlined in Ahmed et al. [2019].

280 6.2 Maximum entropy as a norm-based regularisation on the policy

281 Norm-based complexity measures introduced in Section 4.2 are now evaluated. For a complexity
 282 measure \mathcal{M} to be considered significant, it should be correlated with the robustness of the model.

283 Accordingly, the different norm-based measures presented in Section 4.2 are estimated. Figure 2
 284 shows the layer-wise product norm of the policy actor network parameters ($\mathcal{M}(\pi_\theta, \mathcal{D}) = \prod_{i=1}^l \|\theta_\mu^i\|_p$)
 285 w.r.t. to their associated entropy coefficient α^i for all the 50 independently trained models.

286 Again, policies obtained with initial $\alpha^i > 0$ exhibit a trend toward decreasing complexity measure
 287 values as α increases up to a certain threshold of the entropy coefficient. Similarly to Section 6.1,
 288 the complexity measure continues to decrease after surpassing this threshold for the Lorenz system.
 289 On the other hand, in the KS case, $\mathcal{M}(\pi_\theta, \mathcal{D})$ increases again once its entropy threshold is reached,
 290 notably for the larger entropy coefficient.

291 Moreover, the measures tend to be much more concentrated when $\alpha^i > 0$, especially in the case of
 292 KS (except for the higher α^i).

293 This may indicate that the entropy regularisation acts on the uncertainty of the policy parameters.
 294 Likewise, similar observations can be made for the total norm of the parameters but are not introduced
 295 here for the sake of brevity.

296 Consequently, this experiment highlights an existing correlation between maximum entropy regulari-
 297 sation and norm-based complexity measures. As this complexity measure is linked to the Lipschitz
 298 continuity of the policy, one might wonder if the regularity of the policy is more directly impacted.
 299 This is the purpose of the next subsection.

⁴By replacing the expectation operator \mathbb{E} with the conditional expectation $\mathbb{E}[\cdot | X_0]$ in the definition of \mathcal{R}^π in (3), the quantity becomes a random variable for which the distribution can be estimated by sampling the initial state distribution $X_0 \sim \mathcal{N}(x_e^*, \sigma_e^2 I_d)$. In fact, taking the conditional expectation gives the difference of the standard value functions under P^π and $P^{\pi, \epsilon}$.

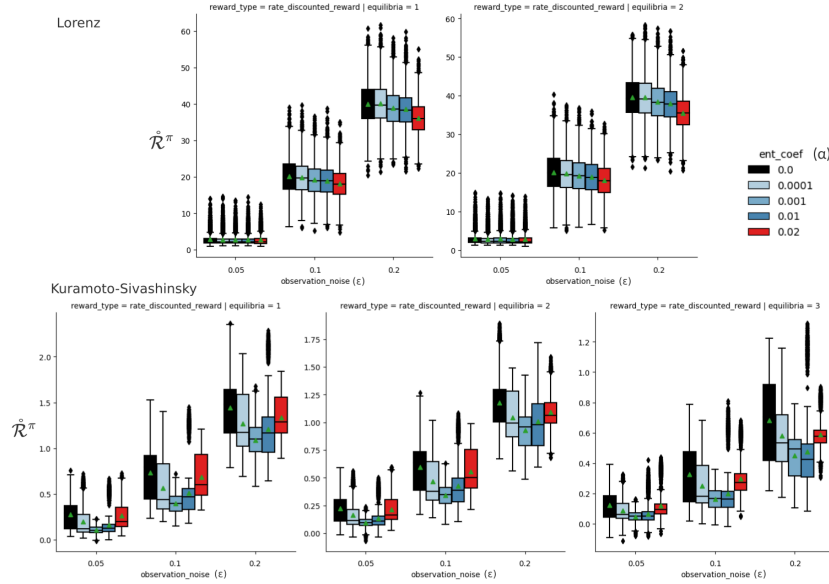


Figure 1: Distributional representation of the rate of excess risk under noise $\hat{\mathcal{R}}^\pi$ conditioned on the α^i used during optimisation for different initial state distribution $X_0 \sim \mathcal{N}(x_e^*, \sigma_e^2 I_d)$. Each of the rows corresponds to one of the dynamical systems of interest. Each of the columns corresponds to one of the initial state distributions of interest. There are two non-zero fixed points (equilibria) x_e^* for Lorenz and three for KS. From top to bottom: KS; Lorenz.

For each box plot, three intensities σ_Y for the observation noise ϵ are evaluated. As expected, when the uncertainty regarding the observable Y increases through the variance σ_Y of the observation signal noise ϵ , the policy performance decreases globally ($\hat{\mathcal{R}}^\pi$ increases). Moreover, the rate of excess risk under noise tends to decrease when α^i increases in the Lorenz case, whereas it decreases up to a certain entropy threshold for KS before increasing again.

300 6.3 Maximum entropy reduces the average Fisher-Information

301 Another regularity measure is considered: the average trace of the Fisher information ($\mathcal{M}(\pi_\theta, \mathcal{D}) =$
 302 $Tr(\mathcal{I}(\theta_\mu)) = Tr(-\mathbb{E}^{X \sim \rho, U \sim \pi_\theta(\cdot | X)} [\nabla_{\theta_\mu}^2 \log \pi_\theta(U | X)])$). As discussed in 4.2.2, this quantity
 303 reflects the regularity of the policy and might be related to the flatness of the local minima of the
 304 objective function.

305 Figure 3 shows the distribution under π_θ of the trace of the state conditional Fisher Information of
 306 the numerical optimal solution θ_{μ, α^i}^* for the policy w.r.t. the α^i used during optimisation. In other
 307 words, a kernel density estimator of the distribution of $Tr(\mathcal{I}(\pi_{\theta^*}(\cdot | X)))$ when $X \sim \rho^{\pi_{\theta^*}}$ is
 308 represented. The results of this experiment suggest first, this distribution is skewed negatively and
 309 has a fat right tail. This means some regions of the support of $\rho^{\pi_{\theta^*}}$ provide FIM trace with extreme
 310 positive values, meaning the regularity of the policy may be poor in these regions of the state space.
 311 A comparison of the distribution w.r.t. the different α^i sheds further light on the relation between
 312 robustness and regularity. In fact, there appears to be a correspondence between the robustness, as
 313 indicated by the rate of excess risk under noise $\hat{\mathcal{R}}^\pi$ shown in Figure 1 and the concentration of the
 314 trace distribution toward larger values (*i.e.* more irregular policies) when the model is less robust.

315 Meanwhile, under the considerations of 4.2.2 and since it is known that entropy regularisation favours
 316 flat minima in RL [Ahmed et al., 2019], these experimental results support the hypothesis of an
 317 existing relationship between robustness, objective function flatness around the solution θ^* and
 318 conditional Fisher information of θ^* .

319 For a complementary point of view, a supplementary experiment regarding the sensitivity of the
 320 policy updates during training w.r.t. to different level of entropy is also presented in Appendix A.

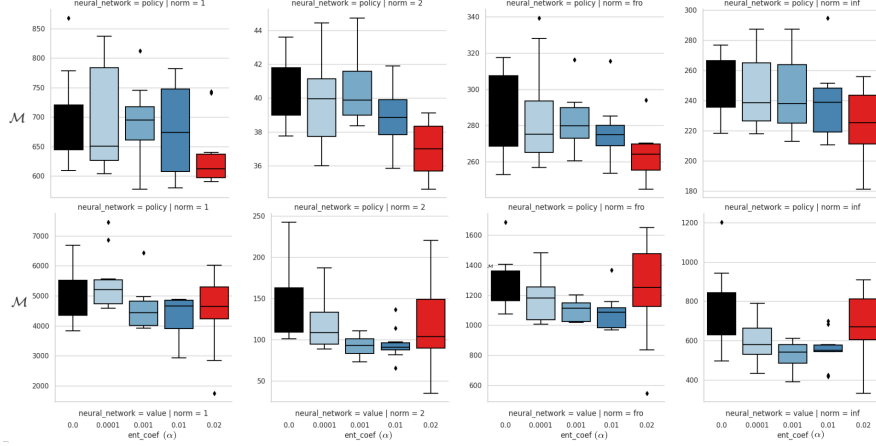


Figure 2: Measures of complexity $\mathcal{M}(\pi_\theta, \mathcal{D}) = \prod_{i=1}^l \|\theta_\mu^i\|_p$ with $p = 1, 2, \infty, F$ conditioned on the α^i used during optimisation. Each row corresponds to one of the dynamical systems of interest while column represents a different norm order p . From top to bottom: Lorenz and KS. For the Lorenz case, the barycenters of the measures tend to decrease when α^i increases. Regarding KS, passing a threshold, the complexity increases again with the entropy. In addition, the measures are much more concentrated when $\alpha^i > 0$. For $p = 2, F$, the separation of the measures w.r.t. the different α^i is more pronounced.

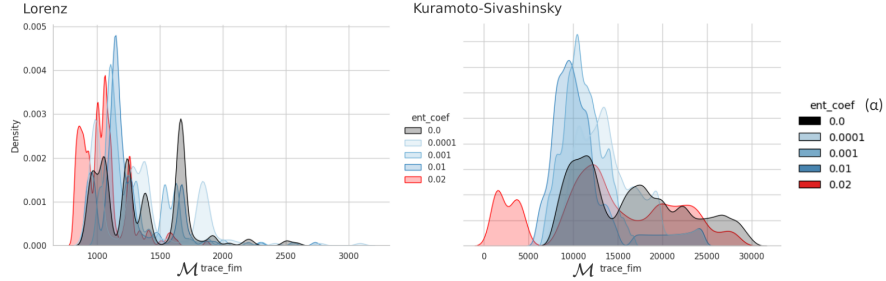


Figure 3: Distribution of the trace of the (conditional) Fisher information of the numerical optimal solution θ_{μ, α^i}^* for the policy w.r.t. the α^i used during optimisation. From left to right: Lorenz and KS environments. Colours: control experiment $\alpha^i = 0$ (black); intermediate entropy level α^i (blue); largest α^i (red).

A skewed distribution towards (relatively) larger values is observed for all controlled dynamical systems. Moreover, those right tails exhibit high kurtosis, especially for the control experiment (black) and the model with the larger entropy coefficient (red) for the KS system. Finally, solutions with intermediate entropy levels (blue) are much more concentrated - have lower variance than the others. About Lorenz, the barycenter of the more robust model (red) is shifted towards lower values than the others.

321 7 Discussion

322 In this paper, the question of the robustness of maximum entropy policies under noise is studied. After
 323 introducing the notion of complexity measures from the statistical learning theory literature, numerical
 324 evidence supports the hypothesis that maximum entropy regularisation induces robustness under
 325 noise. Moreover, norm-based complexity measures are shown to be correlated with the robustness
 326 of the model. Then, the average trace of the Fisher Information is shown to be a relevant indicator
 327 of the regularity of the policy. This suggests the existence of a link between robustness, regularity
 328 and entropy regularisation. Finally, this work contributes to bringing statistical learning concepts
 329 such as flatness into the field of Reinforcement Learning. New algorithms or metrics, such as in the
 330 work of Lecarpentier et al. [2021], may be built upon notions of regularity, *e.g.*, Lipschitz continuity,
 331 flatness or Fisher Information of the parameter in order to achieve robustness.

332 **Acknowledgements**

333 The authors acknowledge the support of the French Agence Nationale de la Recherche (ANR), under
 334 grant ANR-REASON (ANR-21-CE46-0008). This work was performed using HPC resources from
 335 GENCI-IDRIS (Grant 2023-[AD011014278]).

336 **A Weights sensitivity during training**

337 This section is intended to provide complementary insights on the optimisation landscape induced by
 338 the entropy coefficient α during training from the *conservative* or *trust region* policy iteration point
 339 of view Kakade and Langford [2002], Schulman et al. [2015].

340 Let $(\theta_m^\alpha)_{m=1}^{m_D}$ be the sequence of weights of the policy during the training of the model for some initial
 341 entropy coefficient α . The conditional Kullback-Leibler divergence between the policy identified by
 342 the parameters θ_m^α and the subsequent policy defined by the parameters θ_{m+1}^α is given by

$$343 \bar{D}_{KL}(\theta_m^\alpha, \theta_{m+1}^\alpha) = \mathbb{E}^{X \sim \rho} \left[\int_{\mathcal{U}} \log \left(\frac{\pi_{\theta_m^\alpha}(du|X)}{\pi_{\theta_{m+1}^\alpha}(du|X)} \right) \pi_{\theta_{m+1}^\alpha}(du | X) \right].$$

344 The above quantity is a measure of the divergence from the policy at time m to the policy at time
 345 $m + 1$. Thus it may provide information on the local stiffness of the optimisation landscape during
 346 training.

347 Figure 4 shows the evolution of the Kullback-Leibler divergence between two subsequent policies
 348 during training for the Lorenz and KS controlled differential equations. Regarding the Lorenz system,
 349 the maximal divergence is reached for the optimisation performed with the two lowest α^i while
 350 increasing entropy seems to slightly reduce the divergence. On the other hand, the highest divergence
 351 values observed for the KS system are reached for $\alpha^i = 0$ and the maximal entropy coefficient.
 352 This observation is coherent with the results of the previous sections and suggests that the entropy
 353 coefficient α impacts the optimisation landscape during training.

354 Interesting questions regarding the optimisation landscape and its link with the Fisher Information
 355 (through the point of view of Information Geometry [Amari, 1998]) are raised by the results of this
 356 section but are left for future work.

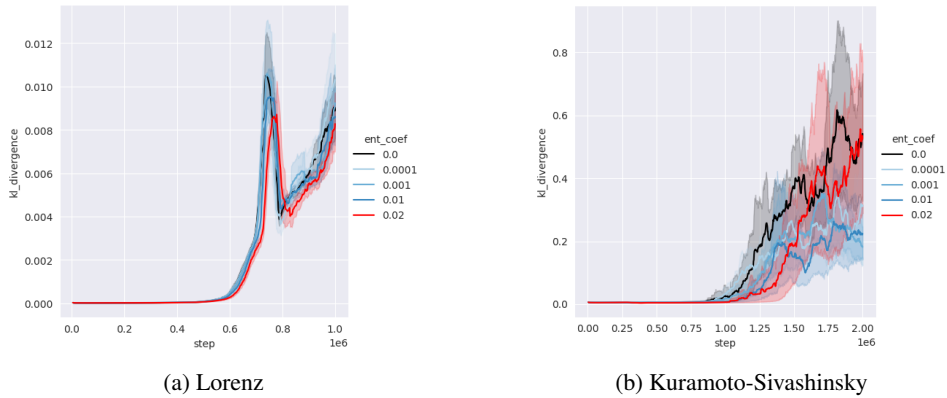


Figure 4: Evolution of $\bar{D}_{KL}(\theta_m^\alpha, \theta_{m+1}^\alpha)$ during training for the Lorenz and KS controlled differential equations. For Lorenz, the maximal divergence is reached for the optimisation performed with $\alpha^i = 0$ and the second lowest α^i . Regarding KS, the highest divergence values are observed for $\alpha^i = 0$ and the maximal entropy coefficient.

357 **References**

358 Ronald J. Williams, Jing Peng, and Hong Li. Function optimization using connectionist reinforcement
 359 learning algorithms. *Connection Science*, 3(3):241–268, 1991.

360 Tuomas Haarnoja, Haoran Tang, Pieter Abbeel, and Sergey Levine. Reinforcement learning with
 361 deep energy-based policies. In Doina Precup and Yee Whye Teh, editors, *Proceedings of the 34th*

- 362 *International Conference on Machine Learning*, volume 70 of *Proceedings of Machine Learning*
363 *Research*, pages 1352–1361. PMLR, 06–11 Aug 2017.
- 364 Olivier Sigaud and Olivier Buffet. *Markov Decision Processes in Artificial Intelligence*. Wiley, 2010.
365 ISBN 978-1-848-21167-4.
- 366 Benjamin Eysenbach and Sergey Levine. Maximum entropy RL (provably) solves some robust RL
367 problems. In *International Conference on Learning Representations, 2022*.
- 368 Tuomas Haarnoja, Aurick Zhou, Pieter Abbeel, and Sergey Levine. Soft actor-critic: Off-policy
369 maximum entropy deep reinforcement learning with a stochastic actor. In Jennifer Dy and Andreas
370 Krause, editors, *Proceedings of the 35th International Conference on Machine Learning*, volume 80
371 of *Proceedings of Machine Learning Research*, pages 1861–1870. PMLR, 10–15 Jul 2018.
- 372 Behnam Neyshabur, Srinadh Bhojanapalli, David Mcallester, and Nati Srebro. Exploring gener-
373 alization in deep learning. In I. Guyon, U. Von Luxburg, S. Bengio, H. Wallach, R. Fergus,
374 S. Vishwanathan, and R. Garnett, editors, *Advances in Neural Information Processing Systems*,
375 volume 30. Curran Associates, Inc., 2017.
- 376 Sepp Hochreiter and Jürgen Schmidhuber. Flat Minima. *Neural Computation*, 9(1):1–42, 01 1997.
377 ISSN 0899-7667.
- 378 Laurent Dinh, Razvan Pascanu, Samy Bengio, and Yoshua Bengio. Sharp minima can generalize
379 for deep nets. In Doina Precup and Yee Whye Teh, editors, *Proceedings of the 34th International*
380 *Conference on Machine Learning*, volume 70 of *Proceedings of Machine Learning Research*, pages
381 1019–1028. PMLR, 06–11 Aug 2017.
- 382 Nitish Shirish Keskar, Jorge Nocedal, Ping Tak Peter Tang, Dheevatsa Mudigere, and Mikhail
383 Smelyanskiy. On large-batch training for deep learning: Generalization gap and sharp minima.
384 2017. 5th International Conference on Learning Representations, ICLR 2017 ; Conference date:
385 24-04-2017 Through 26-04-2017.
- 386 Zafarali Ahmed, Nicolas Le Roux, Mohammad Norouzi, and Dale Schuurmans. Understanding
387 the impact of entropy on policy optimization. In Kamalika Chaudhuri and Ruslan Salakhutdinov,
388 editors, *Proceedings of the 36th International Conference on Machine Learning*, volume 97 of
389 *Proceedings of Machine Learning Research*, pages 151–160. PMLR, 09–15 Jun 2019.
- 390 Gergely Neu, Anders Jonsson, and Vicenç Gómez. A unified view of entropy-regularized markov
391 decision processes. *CoRR*, abs/1705.07798, 2017. URL <http://arxiv.org/abs/1705.07798>.
- 392 Esther Derman, Matthieu Geist, and Shie Mannor. Twice regularized mdps and the equivalence
393 between robustness and regularization. In M. Ranzato, A. Beygelzimer, Y. Dauphin, P.S. Liang,
394 and J. Wortman Vaughan, editors, *Advances in Neural Information Processing Systems*, volume 34,
395 pages 22274–22287. Curran Associates, Inc., 2021.
- 396 David Haussler and Manfred Opper. Mutual information, metric entropy and cumulative relative
397 entropy risk. *The Annals of Statistics*, 25(6):2451–2492, 1997. ISSN 00905364.
- 398 Yang Zhao, Hao Zhang, and Xiuyuan Hu. Penalizing gradient norm for efficiently improving
399 generalization in deep learning. In Kamalika Chaudhuri, Stefanie Jegelka, Le Song, Csaba
400 Szepesvari, Gang Niu, and Sivan Sabato, editors, *Proceedings of the 39th International Conference*
401 *on Machine Learning*, volume 162 of *Proceedings of Machine Learning Research*, pages 26982–
402 26992. PMLR, 17–23 Jul 2022.
- 403 Levent Sagun, Leon Bottou, and Yann LeCun. Eigenvalues of the hessian in deep learning: Singularity
404 and beyond. 2017.
- 405 Yuichi Yoshida and Takeru Miyato. Spectral norm regularization for improving the generalizability
406 of deep learning, 2017.
- 407 Pratik Chaudhari, Anna Choromanska, Stefano Soatto, Yann LeCun, Carlo Baldassi, Christian Borgs,
408 Jennifer Chayes, Levent Sagun, and Riccardo Zecchina. Entropy-sgd: biasing gradient descent
409 into wide valleys*. *Journal of Statistical Mechanics: Theory and Experiment*, 2019(12):124018,
410 dec 2019.

- 411 Florin Gogianu, Tudor Berariu, Mihaela C Rosca, Claudia Clopath, Lucian Busoniu, and Razvan
412 Pascanu. Spectral normalisation for deep reinforcement learning: An optimisation perspective.
413 In Marina Meila and Tong Zhang, editors, *Proceedings of the 38th International Conference on*
414 *Machine Learning*, volume 139 of *Proceedings of Machine Learning Research*, pages 3734–3744.
415 PMLR, 18–24 Jul 2021.
- 416 Jay K. Satia and Roy E. Lave. Markovian decision processes with uncertain transition probabilities.
417 *Operations Research*, 21(3):728–740, 1973. ISSN 0030364X, 15265463. URL <http://www.jstor.org/stable/169381>.
418
- 419 K. Zhou, J.C. Doyle, and K. Glover. *Robust and Optimal Control*. Feher/Prentice Hall Digital and
420 Prentice Hall, 1996. ISBN 9780134565675.
- 421 J. Doyle. Robust and optimal control. In *Proceedings of 35th IEEE Conference on Decision and*
422 *Control*, volume 2, pages 1595–1598 vol.2, 1996.
- 423 Arnab Nilim and Laurent Ghaoui. Robustness in markov decision problems with uncertain transition
424 matrices. In S. Thrun, L. Saul, and B. Schölkopf, editors, *Advances in Neural Information*
425 *Processing Systems*, volume 16. MIT Press, 2003.
- 426 Onésimo Hernández-Lerma and Jean B. Lasserre. *Discrete-Time Markov Control Processes: Basic*
427 *Optimality Criteria*. Springer New York, 1 edition, 1996.
- 428 Marc Peter Deisenroth and Jan Peters. Solving nonlinear continuous state-action-observation pomdps
429 for mechanical systems with gaussian noise. In *European Workshop on Reinforcement Learning*,
430 2012.
- 431 Anthony R. Cassandra. *Exact and Approximate Algorithms for Partially Observable Markov Decision*
432 *Processes*. PhD thesis, Brown University, 1998.
- 433 Thomas M. Cover and Joy A. Thomas. *Elements of Information Theory 2nd Edition (Wiley Series in*
434 *Telecommunications and Signal Processing)*. Wiley-Interscience, July 2006. ISBN 0471241954.
- 435 Behnam Neyshabur, Ryota Tomioka, and Nathan Srebro. Norm-based capacity control in neural
436 networks. In Peter Grünwald, Elad Hazan, and Satyen Kale, editors, *Proceedings of The 28th*
437 *Conference on Learning Theory*, volume 40 of *Proceedings of Machine Learning Research*, pages
438 1376–1401, Paris, France, 03–06 Jul 2015. PMLR.
- 439 Noah Golowich, Alexander Rakhlin, and Ohad Shamir. Size-independent sample complexity of
440 neural networks. In Sébastien Bubeck, Vianney Perchet, and Philippe Rigollet, editors, *Proceedings*
441 *of the 31st Conference On Learning Theory*, volume 75 of *Proceedings of Machine Learning*
442 *Research*, pages 297–299. PMLR, 06–09 Jul 2018.
- 443 Takeru Miyato, Toshiki Kataoka, Masanori Koyama, and Yuichi Yoshida. Spectral normalization for
444 generative adversarial networks. 2018.
- 445 David McAllester. Simplified pac-bayesian margin bounds. In Bernhard Schölkopf and Manfred K.
446 Warmuth, editors, *Learning Theory and Kernel Machines*, pages 203–215, Berlin, Heidelberg,
447 2003. Springer Berlin Heidelberg. ISBN 978-3-540-45167-9.
- 448 Alekh Agarwal, Nan Jiang, and Sham M. Kakade. Reinforcement learning: Theory and algorithms.
449 2019.
- 450 Sham M Kakade. A natural policy gradient. In T. Dietterich, S. Becker, and Z. Ghahramani, editors,
451 *Advances in Neural Information Processing Systems*, volume 14. MIT Press, 2001.
- 452 Zebang Shen, Alejandro Ribeiro, Hamed Hassani, Hui Qian, and Chao Mi. Hessian aided policy
453 gradient. In Kamalika Chaudhuri and Ruslan Salakhutdinov, editors, *Proceedings of the 36th*
454 *International Conference on Machine Learning*, volume 97 of *Proceedings of Machine Learning*
455 *Research*, pages 5729–5738. PMLR, 6 2019.
- 456 Rotem Mulayoff and Tomer Michaeli. Unique properties of flat minima in deep networks. In
457 *Proceedings of the 37th International Conference on Machine Learning*, ICML’20. JMLR.org,
458 2020.

- 459 Zeke Xie, Issei Sato, and Masashi Sugiyama. A diffusion theory for deep learning dynamics:
460 Stochastic gradient descent exponentially favors flat minima. 2021.
- 461 Stanislaw Jastrzebski, Devansh Arpit, Oliver Astrand, Giancarlo B Kerg, Huan Wang, Caiming Xiong,
462 Richard Socher, Kyunghyun Cho, and Krzysztof J Geras. Catastrophic fisher explosion: Early
463 phase fisher matrix impacts generalization. In Marina Meila and Tong Zhang, editors, *Proceedings*
464 *of the 38th International Conference on Machine Learning*, volume 139 of *Proceedings of Machine*
465 *Learning Research*, pages 4772–4784. PMLR, 18–24 Jul 2021.
- 466 Ryo Karakida, Shotaro Akaho, and Shun-ichi Amari. Universal statistics of fisher information in
467 deep neural networks: Mean field approach. In Kamalika Chaudhuri and Masashi Sugiyama,
468 editors, *Proceedings of the Twenty-Second International Conference on Artificial Intelligence and*
469 *Statistics*, volume 89 of *Proceedings of Machine Learning Research*, pages 1032–1041. PMLR,
470 16–18 Apr 2019.
- 471 Peter Henderson, Riashat Islam, Philip Bachman, Joelle Pineau, Doina Precup, and David Meger.
472 Deep reinforcement learning that matters. In *Proceedings of the Thirty-Second AAAI Confer-*
473 *ence on Artificial Intelligence and Thirtieth Innovative Applications of Artificial Intelligence*
474 *Conference and Eighth AAAI Symposium on Educational Advances in Artificial Intelligence*,
475 AAAI’18/IAAI’18/EAAI’18. AAAI Press, 2018. ISBN 978-1-57735-800-8.
- 476 Cédric Colas, Olivier Sigaud, and Pierre-Yves Oudeyer. How many random seeds? statistical power
477 analysis in deep reinforcement learning experiments, 2018.
- 478 Rishabh Agarwal, Max Schwarzer, Pablo Samuel Castro, Aaron C Courville, and Marc Bellemare.
479 Deep reinforcement learning at the edge of the statistical precipice. *Advances in Neural Information*
480 *Processing Systems*, 34, 2021.
- 481 John Schulman, Filip Wolski, Prafulla Dhariwal, Alec Radford, and Oleg Klimov. Proximal policy
482 optimization algorithms. *CoRR*, 2017.
- 483 Thomas L. Vincent and Jianzu Yu. Control of a chaotic system. *Dynamics and Control*, 1(1):35–52,
484 Mar 1991. ISSN 1573-8450.
- 485 M. A. Bucci, O. Semeraro, A. Allauzen, G. Wisniewski, L. Cordier, and L. Mathelin. Con-
486 trol of chaotic systems by deep reinforcement learning. *Proceedings of the Royal Soci-*
487 *ety A: Mathematical, Physical and Engineering Sciences*, 475(2231):20190351, 2019. URL
488 <https://royalsocietypublishing.org/doi/abs/10.1098/rspa.2019.0351>.
- 489 Antonin Raffin, Ashley Hill, Adam Gleave, Anssi Kanervisto, Maximilian Ernestus, and Noah
490 Dormann. Stable-baselines3: Reliable reinforcement learning implementations. *Journal of*
491 *Machine Learning Research*, 22(268):1–8, 2021.
- 492 Erwan Lecarpentier, David Abel, Kavosh Asadi, Yuu Jinnai, Emmanuel Rachelson, and Michael L.
493 Littman. Lipschitz lifelong reinforcement learning, 2021.
- 494 Sham Kakade and John Langford. Approximately optimal approximate reinforcement learning. In
495 *Proceedings of the Nineteenth International Conference on Machine Learning*, ICML ’02, page
496 267–274, San Francisco, CA, USA, 2002. Morgan Kaufmann Publishers Inc. ISBN 1558608737.
- 497 John Schulman, Sergey Levine, Pieter Abbeel, Michael Jordan, and Philipp Moritz. Trust region
498 policy optimization. In Francis Bach and David Blei, editors, *Proceedings of the 32nd International*
499 *Conference on Machine Learning*, volume 37 of *Proceedings of Machine Learning Research*, pages
500 1889–1897, Lille, France, 07–09 Jul 2015. PMLR.
- 501 Shun-ichi Amari. Natural Gradient Works Efficiently in Learning. *Neural Computation*, 10(2):
502 251–276, 02 1998. ISSN 0899-7667. doi: 10.1162/089976698300017746. URL <https://doi.org/10.1162/089976698300017746>.